



Perspectives of seismic imaging using FWI with reciprocity misfit functional

Florian Faucher

► To cite this version:

Florian Faucher. Perspectives of seismic imaging using FWI with reciprocity misfit functional. Journées Ondes Sud-Ouest (JOSO), Mar 2019, Le Barp, France. hal-02076212

HAL Id: hal-02076212

<https://hal.science/hal-02076212>

Submitted on 22 Mar 2019

HAL is a multi-disciplinary open access archive for the deposit and dissemination of scientific research documents, whether they are published or not. The documents may come from teaching and research institutions in France or abroad, or from public or private research centers.

L'archive ouverte pluridisciplinaire **HAL**, est destinée au dépôt et à la diffusion de documents scientifiques de niveau recherche, publiés ou non, émanant des établissements d'enseignement et de recherche français ou étrangers, des laboratoires publics ou privés.

Perspectives of seismic imaging using FWI with reciprocity misfit functional

Florian Faucher¹,

Giovanni Alessandrini², H      Barucq¹, Maarten V. de Hoop³,
Romina Gaburro⁴ and Eva Sincich².

Journ      Ondes Sud-Ouest, CEA Cesta, France

Marth 12th–14th, 2019



¹Project-Team Magique-3D, Inria Bordeaux Sud-Ouest, France.

²Dipartimento di Matematica e Geoscienze, Universit   di Trieste, Italy.

³Department of Computational and Applied Mathematics and Earth Science, Rice University, Houston, USA

⁴Department of Mathematics and Statistics, Health Research Institute (HRI), University of Limerick, Ireland.

Overview

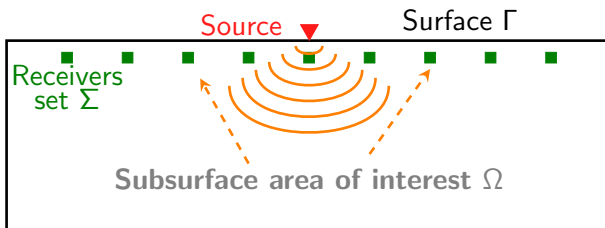
- ① Introduction
- ② Time-Harmonic Inverse Problem, FWI
- ③ Reconstruction procedure using dual-sensors data
- ④ Numerical experiments
 - Comparison of misfit functions
 - Changing the numerical acquisition with $\mathcal{I}_{\mathcal{G}}$
- ⑤ Conclusion

Plan

1 Introduction

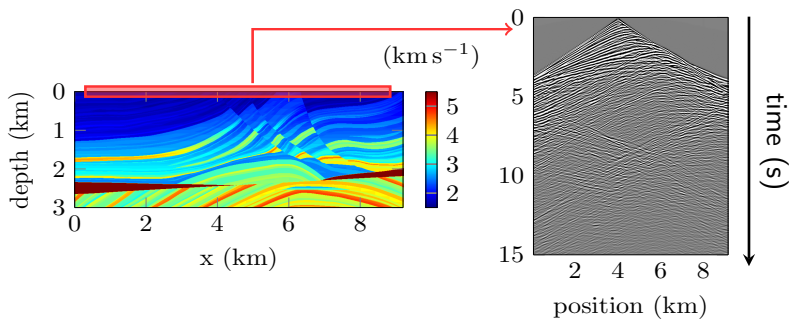
Seismic inverse problem

Reconstruction of subsurface Earth properties from seismic campaign: collection of **wave** propagation data at the surface.



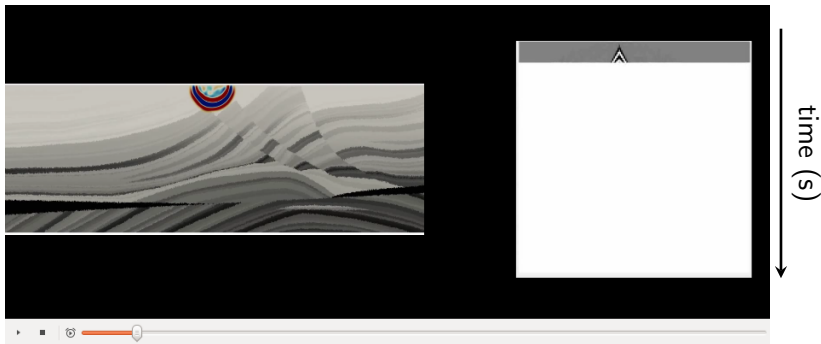
Seismic data

We work with **back-scattered partial data** from **one-side** illumination on large domain.



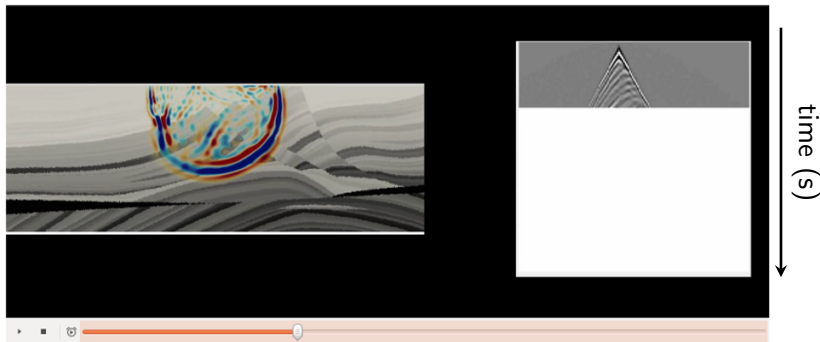
Seismic data

We work with **back-scattered partial data** from **one-side** illumination on large domain.



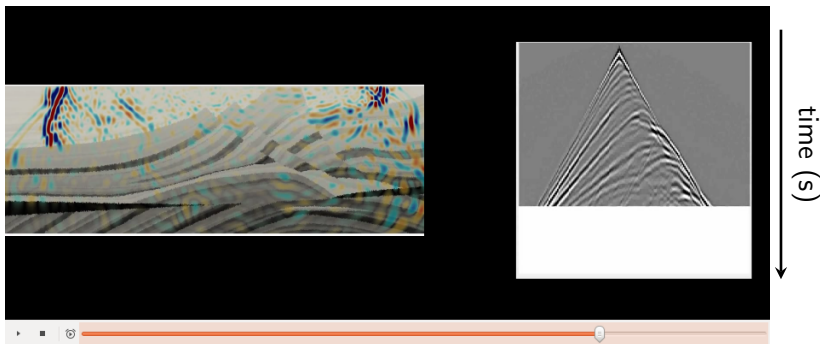
Seismic data

We work with **back-scattered partial data** from **one-side** illumination on large domain.



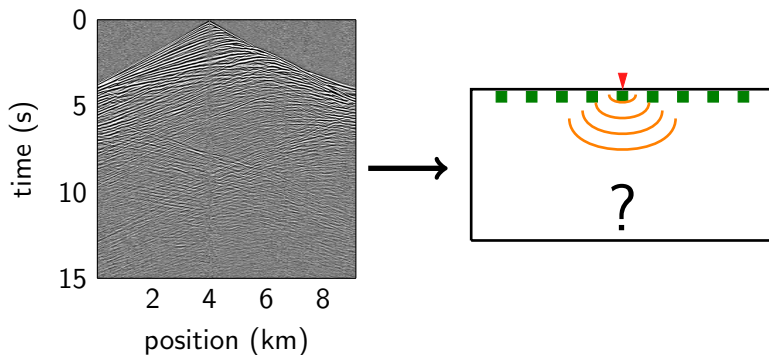
Seismic data

We work with **back-scattered partial data** from **one-side** illumination on large domain.



Seismic data

Inverse problem: from seismic traces to subsurface?



nonlinear, ill-posed inverse problem.

Plan

2 Time-Harmonic Inverse Problem, FWI

Time-harmonic wave equation

We consider propagation in acoustic media, given by the Euler's equations, **heterogeneous** medium parameters κ and ρ :

$$\begin{cases} -i\omega\rho(\mathbf{x})\mathbf{v}(\mathbf{x}) = -\nabla p(\mathbf{x}), \\ -i\omega p(\mathbf{x}) = -\kappa(\mathbf{x})\nabla \cdot \mathbf{v}(\mathbf{x}) + f(\mathbf{x}). \end{cases}$$

p : scalar pressure field,
 \mathbf{v} : vectorial velocity field,
 f : source term,

κ : bulk modulus,
 ρ : density,
 ω : angular frequency.

Time-harmonic wave equation



We consider propagation in acoustic media, given by the Euler's equations, **heterogeneous** medium parameters κ and ρ :

$$\begin{cases} -i\omega\rho(\mathbf{x})\mathbf{v}(\mathbf{x}) = -\nabla p(\mathbf{x}), \\ -i\omega p(\mathbf{x}) = -\kappa(\mathbf{x})\nabla \cdot \mathbf{v}(\mathbf{x}) + f(\mathbf{x}). \end{cases}$$

p : scalar pressure field,

κ : bulk modulus,

\mathbf{v} : vectorial velocity field,

ρ : density,

f : source term,

ω : angular frequency.

The system reduces to the Helmholtz equation when ρ is constant,

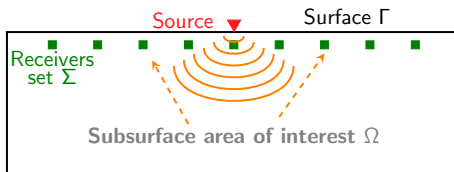
$$(-\omega^2 c(\mathbf{x})^{-2} - \Delta)p(\mathbf{x}) = 0,$$

$$\text{with } c(\mathbf{x}) = \sqrt{\kappa(\mathbf{x})\rho(\mathbf{x})^{-1}}.$$

Dual-sensors devices

The inverse problem aims the recovery of the subsurface medium parameters from surface measurements of pressure **and** normal (vertical) velocity:

$$\mathcal{F} : m = (\kappa, \rho) \rightarrow \{\mathcal{F}_p ; \mathcal{F}_v\} = \{p(\mathbf{x}_1), p(\mathbf{x}_2), \dots, p(\mathbf{x}_{n_{rcv}}); v_n(\mathbf{x}_1), v_n(\mathbf{x}_2), \dots, v_n(\mathbf{x}_{n_{rcv}})\}.$$



D. Carlson, N. D. Whitmore *et al.*

Increased resolution of seismic data from a dual-sensor streamer cable – Imaging of primaries and multiples using a dual-sensor towed streamer

SEG, 2007 – 2010



CGG & Lundun Norway (2017–2018)

TopSeis acquisition (www.cgg.com/en/What-We-Do/Offshore/Products-and-Solutions/TopSeis)

Full Waveform Inversion (FWI)

FWI provides a **quantitative reconstruction** of the subsurface parameters by solving a minimization problem,

$$\min_{m \in \mathcal{M}} \mathcal{J}(m) = \frac{1}{2} \|\mathcal{F}(m) - d\|^2.$$

- ▶ d are the observed data,
- ▶ $\mathcal{F}(m)$ represents the simulation using an initial model m :



[P. Lailly](#)

The seismic inverse problem as a sequence of before stack migrations
[Conference on Inverse Scattering: Theory and Application, SIAM, 1983](#)



[A. Tarantola](#)

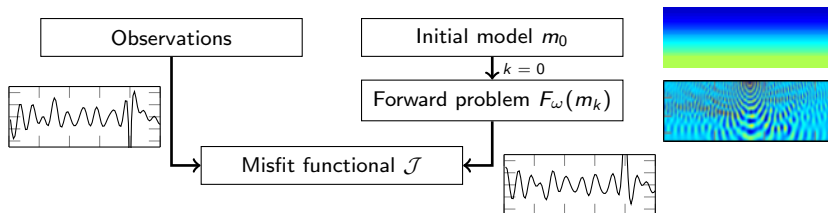
Inversion of seismic reflection data in the acoustic approximation
[Geophysics, 1984](#)



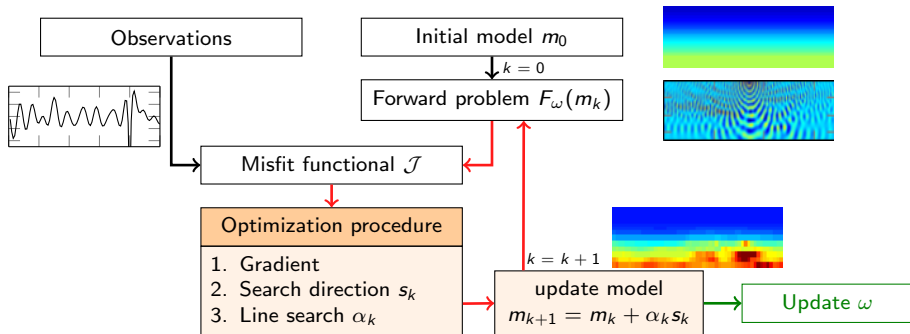
[A. Tarantola](#)

Inversion of travel times and seismic waveforms
[Seismic tomography, 1987](#)

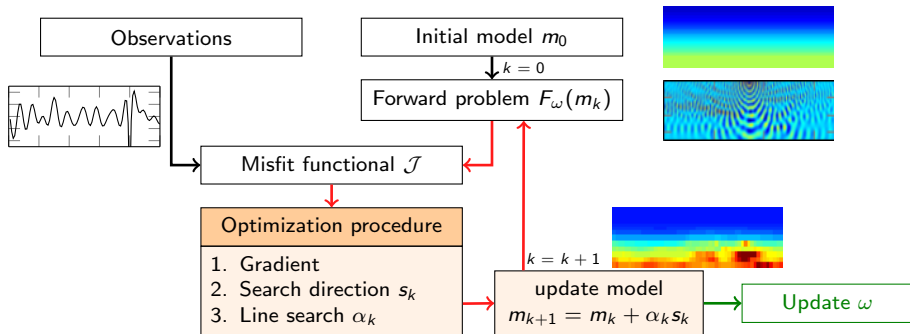
FWI, iterative minimization



FWI, iterative minimization



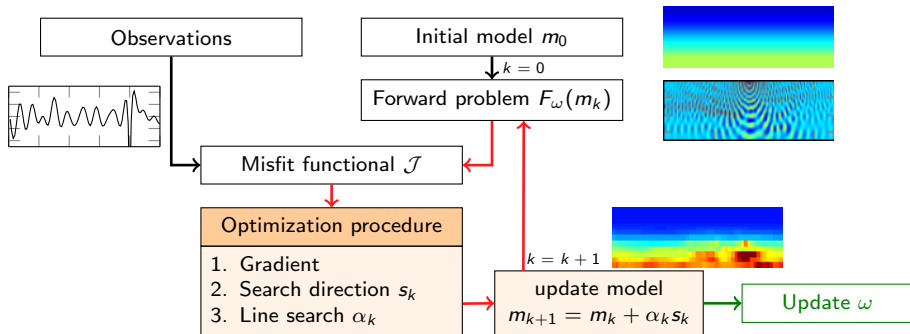
FWI, iterative minimization



Numerical methods

- ▶ Adjoint-method for the gradient computation, L-BFGS method,
- ▶ forward problem resolution with Discontinuous Galerkin methods,
- ▶ parallel computation, HPC, large-scale optimization,
- ▶ Rk: the code also works for **elastic** anisotropy and **viscous** media.

FWI, iterative minimization



- ▶ $> 10^5$: unknowns per physical parameter,
- ▶ $> 10^6$: matrix size for discretization,
- ▶ we also study stability and convergence of the algorithm ...

Plan

3 Reconstruction procedure using dual-sensors data

Minimization of the cost function

The appropriate misfit functional to minimize with pressure and vertical velocity measurements.

- Compare the pressure and velocity fields separately:

$$\mathcal{J}_{L2} = \sum_{source} \frac{1}{2} \|\mathcal{F}_p^{(s)} - d_p^{(s)}\|^2 + \frac{1}{2} \|\mathcal{F}_v^{(s)} - d_v^{(s)}\|^2.$$

Minimization of the cost function

The appropriate misfit functional to minimize with pressure and vertical velocity measurements.

- ▶ Compare the pressure and velocity fields separately:

$$\mathcal{J}_{L2} = \sum_{source} \frac{1}{2} \|\mathcal{F}_p^{(s)} - d_p^{(s)}\|^2 + \frac{1}{2} \|\mathcal{F}_v^{(s)} - d_v^{(s)}\|^2.$$

- ▶ Compare the fields multiplication for all combinations:

$$\mathcal{J}_g = \frac{1}{2} \sum_{s_1} \sum_{s_2} \|d_v^{(s_1)T} \mathcal{F}_p^{(s_2)} - d_p^{(s_1)T} \mathcal{F}_v^{(s_2)}\|^2.$$



G. Alessandrini, M.V. de Hoop, F. F., R. Gaburro and E. Sincich

Inverse problem for the Helmholtz equation with Cauchy data: reconstruction with conditional well-posedness driven iterative regularization

[preprint](#)

Minimization of the cost function

$$\mathcal{J}_{\mathcal{G}} = \frac{1}{2} \sum_{s_1} \sum_{s_2} \|d_v^{(s_1)T} \mathcal{F}_p^{(s_2)} - d_p^{(s_1)T} \mathcal{F}_v^{(s_2)}\|^2.$$

From Euler's equation, $v_n(\mathbf{x}_i) = -i(\omega\rho)^{-1}\partial_n p(\mathbf{x}_i)$.

Minimization of the cost function

$$\mathcal{J}_{\mathcal{G}} = \frac{1}{2} \sum_{s_1} \sum_{s_2} \|d_v^{(s_1)T} \mathcal{F}_p^{(s_2)} - d_p^{(s_1)T} \mathcal{F}_v^{(s_2)}\|^2.$$

From Euler's equation, $v_n(\mathbf{x}_i) = -i(\omega\rho)^{-1}\partial_n p(\mathbf{x}_i)$.

- **Cauchy data:** the cost function follows **Green's identity**.

Minimization of the cost function

$$\mathcal{J}_{\mathcal{G}} = \frac{1}{2} \sum_{s_1} \sum_{s_2} \|d_v^{(s_1)T} \mathcal{F}_p^{(s_2)} - d_p^{(s_1)T} \mathcal{F}_v^{(s_2)}\|^2.$$

From Euler's equation, $v_n(\mathbf{x}_i) = -i(\omega\rho)^{-1}\partial_n p(\mathbf{x}_i)$.

- ▶ **Cauchy data:** the cost function follows **Green's identity**.
- ▶ **Reciprocity gap functional** in inverse scattering.



D. Colton and H. Haddar

An application of the reciprocity gap functional to inverse scattering theory
[Inverse Problems 21 \(1\) \(2005\), 383398.](#)



G. Alessandrini, M.V. de Hoop, R. Gaburro and E. Sincich

Lipschitz stability for a piecewise linear Schrödinger potential from local Cauchy data
[arXiv:1702.04222, 2017](#)



G. Alessandrini, M.V. de Hoop, F. F., R. Gaburro and E. Sincich

Inverse problem for the Helmholtz equation with Cauchy data: reconstruction with conditional well-posedness driven iterative regularization
[preprint](#)

Stability results

Lipschitz type stability is obtained for the Helmholtz equation with partial Cauchy data.

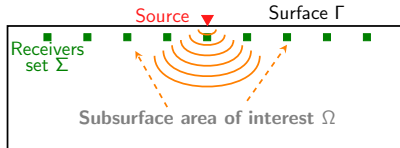
$$\|c_1 - c_2\| \leq \mathcal{C}(\mathcal{J}_{\mathcal{G}}(c_1, c_2))^{1/2}$$

Stability results

Lipschitz type stability is obtained for the Helmholtz equation with **partial Cauchy data**.

$$\|c_1 - c_2\| \leq \mathcal{C}(\mathcal{I}_{\mathcal{G}}(c_1, c_2))^{1/2}$$

- Using back-scattered data from one side in a domain with free surface and absorbing conditions,



- for piecewise linear parameters.



G. Alessandrini, M.V. de Hoop, R. Gaburro and E. Sincich

Lipschitz stability for a piecewise linear Schrödinger potential from local Cauchy data
arXiv:1702.04222, 2017



G. Alessandrini, M.V. de Hoop, F. F., R. Gaburro and E. Sincich

Inverse problem for the Helmholtz equation with Cauchy data: reconstruction with conditional well-posedness driven iterative regularization

Additional possibilities

It allows the non-collocation of numerical and observational sources:

$$\mathcal{J}_{\mathcal{G}} = \frac{1}{2} \sum_{s_1} \sum_{s_2} \|d_v^{(s_1)T} \mathcal{F}_p^{(s_2)} - d_p^{(s_1)T} \mathcal{F}_v^{(s_2)}\|^2.$$

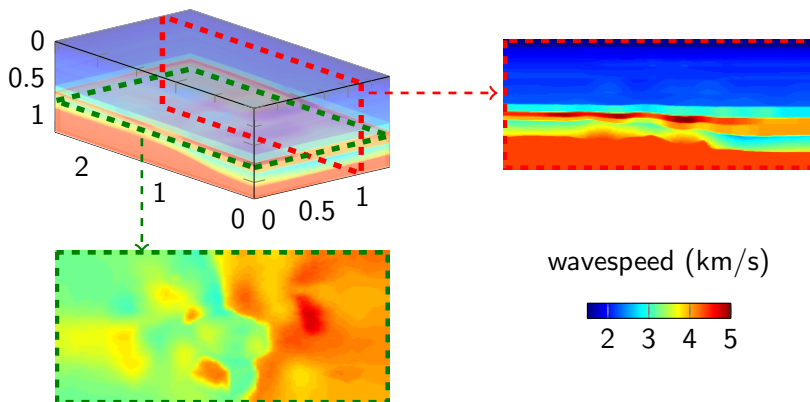
- ▶ s_1 is fixed by the observational setup,
- ▶ s_2 is chosen for the numerical comparisons.

4 Numerical experiments

- Comparison of misfit functions
- Changing the numerical acquisition with \mathcal{I}_g

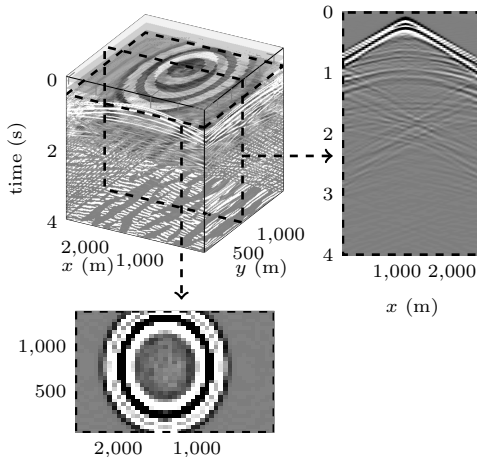
Experiment setup

3D velocity model $2.5 \times 1.5 \times 1.2\text{km}$ using dual-sensors data.



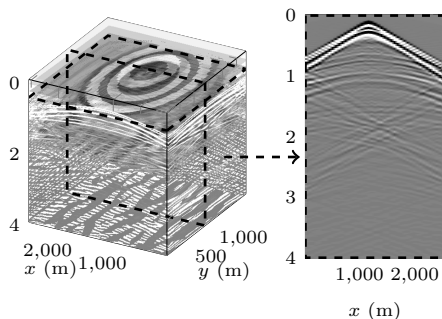
Experiment setup

We work with time-domain data acquisition.



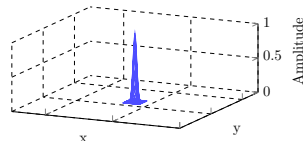
Experiment setup

We work with time-domain data (pressure and velocity).



Acquisition for the measures

- ▶ 160 sources,
- ▶ 100 m depth,
- ▶ point source,



For the reconstruction, we apply a Fourier transform of the time data.

Comparison of misfit functional

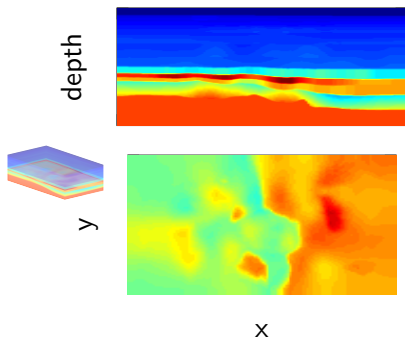
We respect the observational acquisition setup and perform the minimization of \mathcal{J}_{L2} or $\mathcal{J}_{\mathcal{G}}$, frequency from 3 to 15Hz.

$$\mathcal{J}_{L2} = \sum_{source} \frac{1}{2} \|\mathcal{F}_p^{(s)} - d_p^{(s)}\|^2 + \frac{1}{2} \|\mathcal{F}_v^{(s)} - d_v^{(s)}\|^2.$$

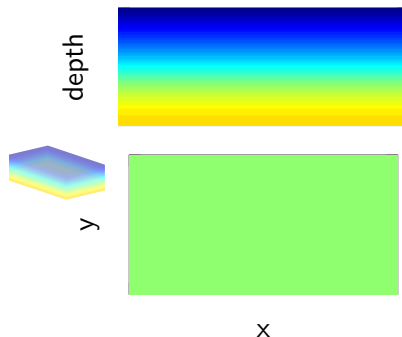
$$\mathcal{J}_{\mathcal{G}} = \frac{1}{2} \sum_{source} \sum_{source} \|d_v^{(s_1)T} \mathcal{F}_p^{(s_2)} - d_p^{(s_1)T} \mathcal{F}_v^{(s_2)}\|^2.$$

Comparison of misfit functional

We respect the observational acquisition setup and perform the minimization of \mathcal{J}_{L2} or $\mathcal{J}_{\mathcal{G}}$, frequency from 3 to 15Hz.



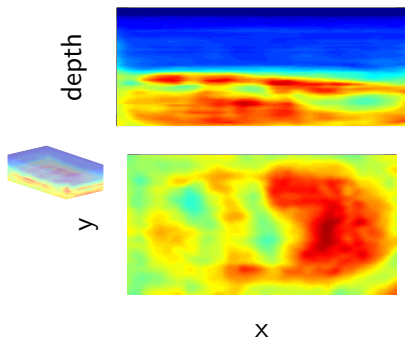
(a) True velocity



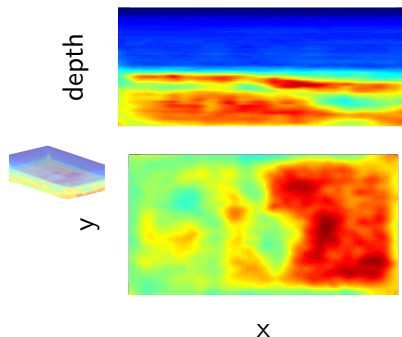
(b) Starting velocity

Comparison of misfit functional

We respect the observational acquisition setup and perform the minimization of \mathcal{J}_{L2} or $\mathcal{J}_{\mathcal{G}}$, frequency from 3 to 15Hz.



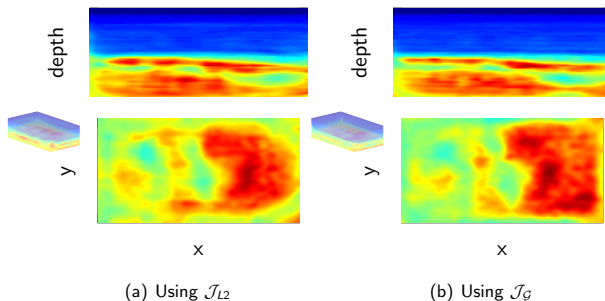
(a) Using \mathcal{J}_{L2}



(b) Using $\mathcal{J}_{\mathcal{G}}$

Comparison of misfit functional

We respect the observational acquisition setup and perform the minimization of \mathcal{J}_{L2} or $\mathcal{J}_{\mathcal{G}}$, frequency from 3 to 15Hz.



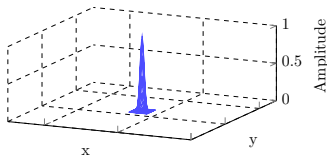
But the major advantage of $\mathcal{J}_{\mathcal{G}}$ is the possibility to consider alternative acquisition setup.

Experiment with different obs. and sim. acquisition *inria* informatics mathematics

$$\min \mathcal{J}_{\mathcal{G}} = \frac{1}{2} \sum_{s_1} \sum_{s_2} \|d_v^{(s_1)T} \mathcal{F}_p^{(s_2)} - d_p^{(s_1)T} \mathcal{F}_v^{(s_2)}\|^2.$$

Acquisition for the measures s_1

- ▶ 160 sources,
- ▶ 100 m depth,
- ▶ point source,

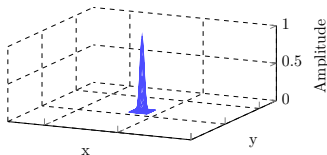


Experiment with different obs. and sim. acquisition

$$\min \mathcal{J}_{\mathcal{G}} = \frac{1}{2} \sum_{s_1} \sum_{s_2} \|d_v^{(s_1)T} \mathcal{F}_p^{(s_2)} - d_p^{(s_1)T} \mathcal{F}_v^{(s_2)}\|^2.$$

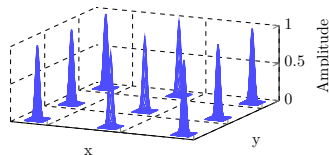
Acquisition for the measures s_1

- ▶ 160 sources,
- ▶ 100 m depth,
- ▶ point source,



Arbitrary numerical acquisition s_2

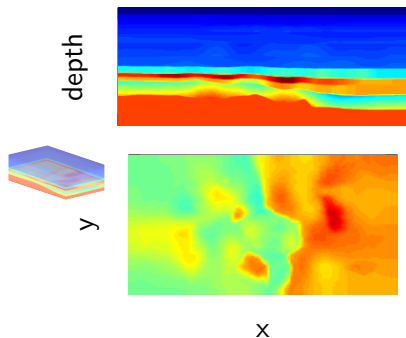
- ▶ **5 sources,**
- ▶ **80m depth,**
- ▶ **multi-point sources,**



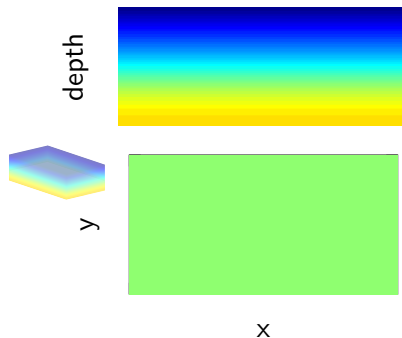
- ▶ No need to know observational source wavelet.
- ▶ Differentiation impossible with least squares types misfit.

Experiment with different obs. and sim. acquisition

Data from frequency between 3 to 15 Hz, domain size $2.5 \times 1.5 \times 1.2$ km, **Simulation using 5 sources only.**



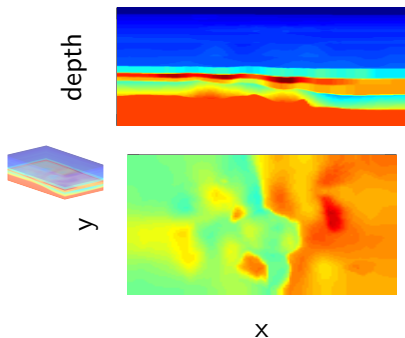
(a) True velocity



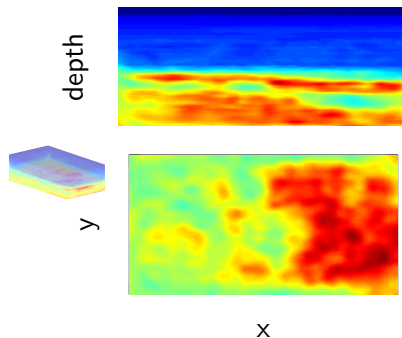
(b) Starting velocity

Experiment with different obs. and sim. acquisition *inria*

Frequency from 3 to 15 Hz, $2.5 \times 1.5 \times 1.2$ km,
Simulation using 5 sources only. -33% computational time.



(a) True velocity



(b) 15 Hz reconstruction

Plan

5 Conclusion

Conclusion



Seismic inverse problem using pressure and vertical velocity data:

- ▶ appropriate cost function to minimize,
- ▶ allow minimal information on the acquisition setup,
- ▶ other applications,
- ▶ **perspective:** design the most efficient numerical setup,
- ▶ Rk: possible for elastic media with measures of traction.

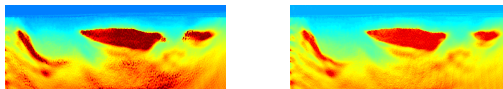
Conclusion

Seismic inverse problem using pressure and vertical velocity data:

- ▶ appropriate cost function to minimize,
- ▶ allow minimal information on the acquisition setup,
- ▶ other applications,
- ▶ **perspective**: design the most efficient numerical setup,
- ▶ **Rk**: possible for elastic media with measures of traction.

Quantitative reconstruction algorithm toolbox for time-harmonic wave,

- ▶ **Discontinuous Galerkin** discretization in HPC framework,
- ▶ large scale optimization scheme using back-scattered data,
- ▶ **acoustic, elastic, anisotropy, 2D, 3D, attenuation**.



P- and S-wavespeed reconstructions

Conclusion

Seismic inverse problem using pressure and vertical velocity data:

- ▶ appropriate cost function to minimize,
- ▶ allow minimal information on the acquisition setup,
- ▶ other applications,
- ▶ **perspective:** design the most efficient numerical setup,
- ▶ Rk: possible for elastic media with measures of traction.

Quantitative reconstruction algorithm toolbox for time-harmonic wave,

- ▶ **Discontinuous Galerkin** discretization in HPC framework,
- ▶ large scale optimization scheme using back-scattered data,
- ▶ **acoustic, elastic, anisotropy, 2D, 3D, attenuation.**

THANK YOU

APPENDIX

$$\|c_1^{-2} - c_2^{-2}\| \leq C(\|F(c_1^{-2}) - F(c_2^{-2})\|)$$



[G. Alessandrini](#)

Stable determination of conductivity by boundary measurement
[Applicable Analysis 1988](#)



[N. Mandache](#)

Exponential instability in an inverse problem for Schrödinger equation
[Inverse Problems 2001](#)

$$\|c_1^{-2} - c_2^{-2}\| \leq C(\|F(c_1^{-2}) - F(c_2^{-2})\|)$$

Diagram illustrating the stability of the Helmholtz inverse problem. The equation shows the difference between the target c_1^{-2} and the initial model c_2^{-2} is bounded by a constant C times the difference between the observation $F(c_1^{-2})$ and the simulation $F(c_2^{-2})$. The error δ is indicated above the observation and simulation terms.

- ▶ Stability associate data and model correspondence
- ▶ Reconstruction is based on the iterative minimization of the difference between observation and simulation using an initial model.



G. Alessandrini

Stable determination of conductivity by boundary measurement
Applicable Analysis 1988



N. Mandache

Exponential instability in an inverse problem for Schrödinger equation
Inverse Problems 2001

$$\|c_1^{-2} - c_2^{-2}\| \leq C(\|F(c_1^{-2}) - F(c_2^{-2})\|)$$

Diagram illustrating the stability of the Helmholtz inverse problem. The equation shows the difference in the squared inverse of the coefficients, $\|c_1^{-2} - c_2^{-2}\|$, bounded by a constant C times the difference in the forward problem, $\|F(c_1^{-2}) - F(c_2^{-2})\|$. The forward problem difference is labeled with a bracket as δ . Arrows indicate the mapping from the labels to the terms in the equation:

- target** (blue) points to c_1^{-2}
- initial model** (red) points to c_2^{-2}
- observation** (blue) points to $F(c_1^{-2})$
- simulation** (red) points to $F(c_2^{-2})$

- ▶ Stability associate data and model correspondence
- ▶ $C(\delta) \leq C(\log(1 + \delta^{-1}))^{-\alpha}$



G. Alessandrini

Stable determination of conductivity by boundary measurement
Applicable Analysis 1988



N. Mandache

Exponential instability in an inverse problem for Schrödinger equation
Inverse Problems 2001

- ▶ $c(x)$ is bounded $B_1 \leq c^{-2}(x) \leq B_2$ in Ω
- ▶ $c(x)$ has a **piecewise constant** representation of size N

$$c(x)^{-2} = \sum_{k=1}^N c_k \chi_k(x)$$

- ▶ Ω has Lipschitz boundary

$$\|c_1^{-2} - c_2^{-2}\|_{L^2(\Omega)} \leq \mathcal{C} \|F(c_1^{-2}) - F(c_2^{-2})\| \quad (1)$$



G. Alessandrini and S. Vessella

Lipschitz stability for the inverse conductivity problem
[Advances in Applied Mathematics 2005](#)



E. Beretta, M. V. de Hoop, F. and O. Scherzer

Inverse boundary value problem for the Helmholtz equation: quantitative conditional Lipschitz stability estimates.

[SIAM Journal of Mathematical Analysis 2016](#)

The stability constant is bounded

$$\frac{1}{4\omega^2} e^{K_1 N^{1/5}} \leq \mathcal{C} \leq \frac{1}{\omega^2} e^{(K(1+\omega^2 B_2) N^{4/7})} \quad (2)$$

- depends on the partitioning N and the frequency ω



E. Beretta, M. V. de Hoop, F. and O. Scherzer

Inverse boundary value problem for the Helmholtz equation: quantitative conditional Lipschitz stability estimates [2016](#)

In the case of partial Cauchy data (p and $\partial_\nu p$), we have that, we can obtain a Lipschitz type stability:

$$\|c_1^{-2} - c_2^{-2}\| \leq \mathcal{C}(\mathcal{I}_G(c_1^{-2}, c_2^{-2}))^{1/2}$$

Where c_1^{-2} and c_2^{-2} are piecewise linear.